A Hexairon(III) Complex with Three Nonplanar η^2-μ^4-Peroxo Ligands Bridging Two Basic Iron Acetate Units

Itzhak Shweky,[1a] Laura E. Pence,[1b] Georgia C. Papaefthymiou,[1c] Roberta Sessoli,[1d] Joanne W. Yun,[1b] Avi Bino,*[,1a] and Stephen J. Lippard*[,1b]

Contribution from the Department of Inorganic and Analytical Chemistry, Hebrew University of Jerusalem, 91904 Jerusalem, Israel, Department of Chemistry and Francis Bitter Magnet Laboratory, Massachusetts Institute of Technology, Cambridge, Massachusetts 02139, and Dipartimento di Chimica, Universitá degli Studi di Firenze, Firenze, Italia 50144

Received August 30, 1996[⊗]

Abstract: The novel η^2-μ^4-peroxo hexairon(III) complex, $[Fe_6(O)_2(O_2)_3(OAc)_9]^-$, was prepared as its $[Fe_3O(OAc)_6(H_2O)_3]^+$ salt by addition of H_2O_2 to basic iron acetate in the presence of $NaOCH_3$. The compound $[Fe_3O(OAc)_6(H_2O)_3][Fe_6(O)_2(O_2)_3(OAc)_9]\cdot 8H_2O$ crystallizes in the hexagonal space group, $P6_3/m$ with unit cell parameters of $a = 14.276(5)$, $c = 18.935(3)$ Å, $V = 3342.0(1)$ Å^3, and $Z = 2$; the structure was solved and refined to a final residual of $R = 0.044$. The anionic component of the salt contains two trinuclear $\{Fe_3O\}^{7+}$ units arranged in a face-to-face manner. The resulting trigonal prism has η^2-μ^4-peroxo ligands bridging each rectangular face and η^2-μ^2-acetates bridging each edge of the rectangular and triangular faces. Two distinguishing structural features are an elongated O−O bond distance of 1.472(9) Å for the bridging peroxo ligand and significant displacement of this group by 1.05 Å out of the plane of the four iron atoms that it links. The ν_{O-O} stretching mode is readily observed by Raman spectroscopy at 844 cm^{-1}, as in other peroxo-bridged polyiron(III) complexes, but the UV−visible spectrum lacks the distinctive charge transfer band in the 500−800 nm region found in most other ferric peroxo species. Mössbauer isomer shift and quadrupole splitting parameters at 4.2 K are $\delta = 0.51$ and 0.53 mm/s and $\Delta E_q = 1.16$ and 0.79 mm/s for the cation and anionic iron clusters, respectively. Asymmetric line broadening indicated the onset of slow spin relaxation at the lowest temperatures (4.2 K). Variable temperature magnetic susceptibility data measured on a solid sample of $[Fe_3O(OAc)_6(H_2O)_3][Fe_6(O)_2(O_2)_3(OAc)_9]$ revealed antiferromagnetic coupling within the $\{Fe_3O\}^{7+}$ units ($J \sim -30$ to -50 cm^{-1}) and weak ferromagnetic coupling ($J \sim 1$ cm^{-1}) through the η^2-μ^4-peroxo bridges, where $H = -2J|S_i \cdot S_j|$.

Introduction

Carboxylate-bridged diiron(II) centers react with dioxygen to form peroxodiiron(III) intermediates in the catalytic cycle of a variety of nonheme iron proteins including methane monooxygenase and ribonucleotide reductase. Understanding the structure and reactivity of these species, both in the proteins and in synthetic model complexes, is a subject of considerable current attention.[2,3] Recent kinetic studies have revealed that, outside the environment of a protein active site, peroxodiiron(III) species generated in this fashion react in a bimolecular manner with the diiron(II) precursor to form stable (μ-oxo)diiron(III) end products incapable of undergoing biomimetic reaction chemistry.[4,5] This redox transformation was postulated to traverse an (η^2-μ^4-peroxo)tetrairon(II,II,III,III) transition state for which there was some geometric precedence in the structurally characterized complex $[Fe_6O_2(O_2)(O_2CPh)_{12}(H_2O)_2]$.[6] This hexairon(III) compound was the only iron peroxo complex to have been crystallographically identified until this year, when the X-ray structures of three metastable (μ-peroxo)diiron(III) complexes were reported.[7−9]

Apart from their value as models for the reaction of nonheme iron centers with O_2 and H_2O_2, polymetallic peroxo and oxo complexes of iron may provide insight into the nature of, and intermediates in the formation of, the mineral core of the iron storage protein ferritin.[10−13] The probable building blocks of the iron/oxygen network within the ferritin core are most likely found among the common structural motifs observed in synthetic iron chemistry.[14−16] Of the recurring structural units, $\{Fe_2O\}^{4+}$, $\{Fe_3O\}^{7+}$, $\{Fe_4O_2\}^{8+}$, and $\{Fe_6O\}^{16+}$,[6,17−29] it is the basic iron carboxylate unit, $\{Fe_3O\}^{7+}$, that has been widely found to be

⊗ Abstract published in *Advance ACS Abstracts,* January 15, 1997.

(1) (a) Department of Inorganic and Analytical Chemistry, Hebrew University of Jerusalem. (b) Department of Chemistry, Massachusetts Institute of Technology. (c) Francis Bitter Magnet Laboratory, Massachusetts Institute of Technology. (d) Dipartimento di Chimica, Universitá degli Studi di Firenze.

(2) Feig, A. L.; Lippard, S. J. *Chem. Rev.* **1994**, *94*, 759−805.
(3) Que, L., Jr.; Dong, Y. *Acc. Chem. Res.* **1996**, *29*, 190−196.
(4) Feig, A. L.; Becker, M.; Schindler, S.; van Eldik, R.; Lippard, S. J. *Inorg.Chem.* **1996**, *35*, 2590−2601.
(5) Feig, A. L.; Masschelein, A.; Bakac, A.; Lippard, S. J. *J. Am. Chem. Soc.* **1997**, *119*, 334−342.
(6) Micklitz, W.; Bott, S. G.; Bentsen, J. G.; Lippard, S. J. *J. Am. Chem. Soc.* **1989**, *111*, 372−374.
(7) Kim, K.; Lippard, S. J. *J. Am. Chem. Soc.* **1996**, *118*, 4914−4915.
(8) Ookubo, T.; Sugimoto, H.; Nagayama, T.; Masuda, H.; Sato, T.; Tanaka, K.; Maeda, Y.; Okawa, H.; Hayashi, Y.; Uehara, A.; Suzuki, M. *J. Am. Chem. Soc.* **1996**, *118*, 701−702.
(9) Dong, Y.; Yan, S.; Young, V. G., Jr.; Que, L., Jr. *Angew. Chem., Int. Ed. Engl.* **1996**, *35*, 618−620.
(10) Theil, E. C. In *Advances in Enzymology and Related Areas of Molecular Biology*; Meister, A., Ed.; John Wiley: New York, 1990; Vol. 63, pp 421−450.
(11) Lippard, S. J. *Angew. Chem., Int. Ed. Engl* **1988**, *27*, 344−361.
(12) Harrison, P. M.; Lilley, T. H. In *Iron Carriers and Iron Proteins*; Loehr, T. M., Ed.; VCH: New York, 1989; Vol. 5, pp 123−238.
(13) Heath, S. L.; Charnock, J. M.; Garner, C. D.; Powell, A. K. *Chem. Eur. J.* **1996**, *2*, 634−639.
(14) Micklitz, W.; McKee, V.; Rardin, R. L.; Pence, L. E.; Papaefthymiou, G. C.; Bott, S. G.; Lippard, S. J. *J. Am. Chem. Soc.* **1994**, *116*, 8061−8069.
(15) Hagen, K. S. *Angew. Chem., Int. Ed. Engl.* **1992**, *31*, 1010−1012.
(16) Lippard, S. J. *Chem. Br.* **1986**, *22*, 221−228.
(17) Micklitz, W.; Lippard, S. J. *Inorg. Chem.* **1988**, *27*, 3067−3069.
(18) Gorun, S. M.; Papaefthymiou, G. C.; Frankel, R. B.; Lippard, S. J. *J. Am. Chem. Soc.* **1987**, *109*, 3337−3348.
(19) Heath, S. L.; Powell, A. K. *Angew. Chem., Int. Ed. Engl.* **1992**, *31*, 191−193.
(20) Gorun, S. M.; Lippard, S. J. *Inorg. Chem.* **1988**, *27*, 149−156.
(21) Armstrong, W. H.; Roth, M. E.; Lippard, S. J. *J. Am. Chem. Soc.* **1987**, *109*, 6318−6326.

S0002-7863(96)03062-4 CCC: $14.00

present as either a starting material for, or structural motif in, larger iron clusters. Clusters of nuclearity Fe_6,[6,17] Fe_{10},[30] Fe_{11},[18] and Fe_{17}[14] have been prepared by using basic iron carboxylates as the starting materials. Other syntheses do not employ starting materials containing the $\{Fe_3O\}^{7+}$ unit, but the triangular structure is found in the product.[19−23] Continued exploration of this chemistry will potentially produce models of ferritin intermediates as well as provide compounds that bridge the boundaries of the molecular and the solid state.[14,18]

Previously, we reported two specific examples of hexanuclear clusters having $\{Fe_3O\}^{7+}$ basic iron acetates linked in an edge-to-edge fashion. Either a η^2-μ^4-peroxo or two hydroxo ligands bridged the two triiron units in $[Fe_6O_2(O_2)(O_2CPh)_{12}(H_2O)_2]$ and $[Fe_6O_2(OH)_2(O_2CPh)_{12}(H_2O)(1,4\text{-dioxane})]$, respectively.[6,17] Efforts to interconvert the two species and provide a practical model for aspects of the oxygen-evolving complex of photosystem II, where water is converted to dioxygen,[31,32] revealed exchange with H_2O_2 rather than oxidative coupling of the hydroxide ligands. This investigation, however, highlighted the importance of structural models for peroxide and other intermediates postulated for the oxidation of water to dioxygen.[32−36] As already mentioned, stable peroxo adducts of iron(III) in the absence of porphyrin ligands are few and, even in manganese chemistry, only a handful of stable peroxo complexes have been characterized.[35,37−42]

In the present article, we describe a novel hexanuclear iron cluster which contains three peroxo ligands bound in an unusual out-of-plane η^2-μ^4 arrangement. The species, $[Fe_6(O)_2(O_2)_3(OAc)_9]^-$, is prepared from basic iron acetate, and the product contains two $\{Fe_3O\}^{7+}$ units in a face-to-face arrangement bridged by both peroxo ligands and acetates. The results of X-ray crystallographic, Mössbauer, Raman, and magnetic studies are also detailed.

Table 1. Experimental Details of the X-ray Diffraction Studies of $[Fe_3(O)(OAc)_6(H_2O)_3][Fe_6(O)_2(O_2)_3(OAc)_9]\cdot 8H_2O$

compound	**1**·8H_2O[a]
formula	$C_{30}H_{67}Fe_9O_{50}$
formula weight, g mol^{-1}	1730.49
crystal system	hexagonal
space group	$P6_3/m$
a, Å	14.276(5)
c, Å	18.935(3)
V, Å^3	3342.0(1)
Z	2
T, deg C	−89.5
ρ_{calcd}, g cm^{-3}	1.720
crystal dimensions, mm	0.30 × 0.30 × 0.50
transmission factor range	0.912−1.000
crystal decay	0%
linear abs coeff, cm^{-1}	19.9
data collected	$3° \le 2\theta \le 50°$; $+h, +k, +l$
reflections collected	2573
R_{avg} for refl averaging	0.03
no. of independent data	2089
no. of unique data with $I > 3\sigma(I)$	1324
no. of variables	140
R_1[b]	0.044
GOF[c]	1.125

[a] Data collected on an Enraf-Nonius CAD4 kappa geometry diffractometer with graphite monochromatized Mo K$\bar{\alpha}$ radiation ($\bar{\lambda}$ = 0.71073 Å). [b] $R = \sum||F_o| - |F_c||/\sum|F_o|$. [c] GOF = $[\sum w(F_o^2 - F_c^2)^2]/(n - p)]^{1/2}$, where n and p denote the number of data and parameters.

Experimental Section

General Procedures. $[Fe_3O(OAc)_6(H_2O)_3](NO_3)$ was prepared by a literature procedure.[43] Solvents and reagents were used as received from commercial sources.

Preparation of $[Fe_3O(OAc)_6(H_2O)_3][Fe_6(O)_2(O_2)_3(OAc)_9]$, 1. To a solution of basic iron acetate, $[Fe_3O(OAc)_6(H_2O)_3](NO_3)$ (0.10 g, 0.15 mmol) in CH_3CN (5 mL) were added $NaOCH_3$ (0.010 g, 0.18 mmol) and two drops of 30% H_2O_2. The solution was stirred at room temperature for 10 min, filtered, and allowed to stand for slow evaporation. Dark brown crystals of **1** were obtained in 7−10% yield after several days. The crystals were collected and washed with acetone and diethyl ether. IR (KBr, cm^{-1}): 3426 m, br, 3192 w, br, 3025 w, 2928 w, 2853 w, 1587 vs, 1558 vs, 1445 vs, 1384 vs, 1350 w, 1049 m, 1028 m, 948 w, 837 w, 756 w, 660 s, 639 m, 615 s, 529 w, 474 w. Electronic spectrum in CH_3CN: 425 (sh), 460 (sh), 490 (sh) nm. Anal. Calcd for $Fe_9C_{32}NO_{48}H_{60}$, **1**·6H_2O·CH_3CN: C, 22.22; H, 3.5; Fe, 29.06. Found: C, 22.15; H, 3.83; Fe 28.96.

X-ray Crystallography. X-ray quality crystals of **1**·8H_2O were obtained by slow evaporation of a solution of the compound in acetone. A brown hexagonal rod of approximate dimensions 0.30 × 0.30 × 0.50 mm was mounted with grease on the end of a quartz fiber. Unit cell and intensity data were collected by methods standard in our laboratory,[44] the details of which are recorded in Table 1. The hexagonal 6/m symmetry was confirmed both by axial photographs and by the automatic Laue check included in the CAD4-Express software package.[45] All aspects of the structure solution and refinement were handled by the SHELXTL version 5.0 software package.[46] The lattice solvents were located through the application of alternating cycles of least-squares refinement and difference Fourier maps. One interstitial water molecule was refined at partial occupancy over two positions to fit the electron density satisfactorily. All nonhydrogen atoms were refined anisotropically. Hydrogen atoms bonded to carbon were included at calculated positions. The largest peak in the final difference map was 0.9 e$^-$/Å^3, located near the disordered lattice water molecule.

(22) Wieghardt, K.; Pohl, K.; Jibril, I.; Huttner, G. *Angew. Chem., Int. Ed. Engl.* **1984**, *23*, 77−78.
(23) Gérbéléu, N. V.; Batsanov, A. S.; Timko, G. A.; Struchkov, Y. T.; Indrichan, K. M.; Popovich, G. A. *Dokl. Akad. Nauk SSSR* **1986**, *293*, 364−367.
(24) Taft, K. L.; Papaefthymiou, G. C.; Lippard, S. J. *Science* **1993**, *259*, 1302−1305.
(25) Taft, K. L.; Papaefthymiou, G. C.; Lippard, S. J. *Inorg. Chem.* **1994**, *33*, 1510−1520.
(26) Hegetschweiler, K.; Schmalle, H. W.; Streit, H. M.; Gramlich, V.; Hund, H.-U.; Erni, I. *Inorg. Chem.* **1992**, *31*, 1299−1302.
(27) Nair, V. S.; Hagen, K. S. *Inorg. Chem.* **1992**, *31*, 4048−4050.
(28) Gorun, S. M.; Papaefthymiou, G. C.; Frankel, R. B.; Lippard, S. J. *J. Am. Chem. Soc.* **1987**, *109*, 4244−4255.
(29) Jameson, D. L.; Xie, C.-L.; Hendrickson, D. N.; Potenza, J. A.; Schugar, H. J. *J. Am. Chem. Soc.* **1987**, *109*, 740−746.
(30) Taft, K. L.; Lippard, S. J. *J. Am. Chem. Soc.* **1990**, *112*, 9629−9630.
(31) Debus, R. J. *Biochim. Biophys. Acta* **1992**, *1102*, 269−352.
(32) Renger, G. *Angew. Chem., Int. Ed. Engl.* **1987**, *26*, 643−660.
(33) Gilbert, J. A.; Eggleston, D. S. ; Murphy, W. R. Jr.; Geselowitz, D. A.; Gersten, S. W.; Hodgson, D. J.; Meyer, T. J. *J. Am. Chem. Soc.* **1985**, *107*, 3855−3864.
(34) Brudvig, G. W.; Crabtree, R. H. *Proc. Natl. Acad. Sci. U.S.A.* **1986**, *83*, 4586−4588.
(35) Pecoraro, V. L.; Baldwin, M. J.; Gelasco, A. *Chem. Rev.* **1994**, *94*, 807−826.
(36) Kambara, T.; Govindjee *Proc. Natl. Acad. Sci. U.S.A.* **1985**, *82*, 6119−6123.
(37) Kitajima, N.; Komatsuzaki, H.; Hikichi, S.; Osawa, M.; Moro-oka, Y. *J. Am. Chem. Soc.* **1994**, *116*, 11596−11597.
(38) Kitajima, N.; Singh, U. P.; Amagai, H.; Osawa, M.; Moro-oka, Y. *J. Am. Chem. Soc.* **1991**, *113*, 7757−7758.
(39) Bossek, U.; Weyhermüller, T.; Wieghardt, K. *J. Inorg. Biochem.* **1991**, *43*, 371.
(40) Bossek, U.; Weyhermüller, T.; Wieghardt, K.; Nuber, B.; Weiss, J. *J. Am. Chem. Soc.* **1990**, *112*, 6387−6388.
(41) Bhula, R.; Gainsford, G. J.; Weatherburn, D. C. *J. Am. Chem. Soc.* **1988**, *110*, 7550−7552.
(42) VanAtta, R. B.; Strouse, C. E.; Hanson, L. K.; Valentine, J. S. *J. Am. Chem. Soc.* **1987**, *109*, 1425−1434.
(43) Duncan, J. F.; Kanekar, C. R.; Mok, K. F. *J. Chem. Soc. A* **1969**, 480−482.
(44) Carnahan, E. M.; Rardin, R. L.; Bott, S. G.; Lippard, S. J. *Inorg. Chem.* **1992**, *31*, 5193−5201.
(45) CAD4-Express, Version 1.1; Delft Instruments; Delft, The Netherlands, 1992.
(46) Sheldrick, G. M., Siemens Industrial Automation, Inc.; Analytical Instrumentation: Madison, WI, 1994.

Scheme 1

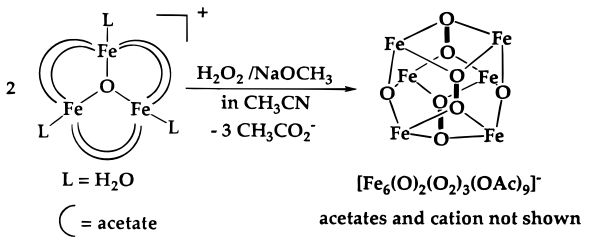

Physical Measurements. Fourier transform infrared spectra of KBr pellets were recorded on a Bio-Rad SPC3200 spectrophotometer and UV−visible spectra on a Perkin Elmer Lambda 7 or Hewlett Packard 8452A Diode Array spectrophotometer.

Mössbauer data were collected by using a conventional Mössbauer spectrometer. The source was ^{57}Co(Rh) maintained at room temperature. The velocity scale of the spectrometer was calibrated by using a thin iron foil with zero velocity at the center of a pure iron spectrum. Isomer shifts were referenced to iron metal at room temperature. The sample temperature was varied by using a Janis Research Superveritemp dewar and a Lakeshore Cryotronics temperature controller.

Solid-state magnetic measurements of **1** were made by using a Metronique MS02 SQUID susceptometer located at the University of Florence. More than 45 data points between 5 and 300 K were collected at 3 kG. The magnetism of the sample holders was measured at the same fields and temperatures and subtracted from the experimental values. A diamagnetic correction of -791×10^{-6} emu mol^{-1} was calculated from Pascal's constants and applied.[47,48]

Raman spectra were obtained by using a Coherent Innova 70 argon ion laser with an excitation wavelength of 514.5 nm and approximately 100 mW of power. A 0.6 m single monochromator (grating, 1200 grooves/mm) with an entrance slit of 100 μm and a liquid-nitrogen-cooled CCD detector (Princeton Instruments, Inc., #LNCCD-512TK) were used in a standard backscattering configuration. A holographic notch filter (Kaiser Optical Systems) was used to attenuate Rayleigh scattering. A 5 mM solution of **1** was prepared in acetonitrile. Spectra were recorded at room temperature, and a total of 10 scans were taken at a rate of approximately 1 scan/s. The data were processed using CSMA software (Princeton Instruments, Inc. Version 2.4A) on a Gateway 2000 computer.

Results and Discussion

Synthesis. The formation of a hexanuclear cluster containing two oxo-bridged trinuclear metal units bridged by either peroxide or hydroxides has been demonstrated for both iron and titanium.[6,17,23,49] In the case of the peroxo-bridged hexairon(III) compound, $[Fe_6(O)_2(O_2)(O_2CPh)_{12}(H_2O)_2]$, the product was formed by the addition of hydrogen peroxide to a slurry of basic iron acetate.[6] The formation of **1** from a similar reaction was facilitated by addition of $NaOCH_3$ to the reaction solution. The additional base increased the extent to which H_2O_2 was deprotonated, and the resulting compound contained three peroxo bridges rather than one. The use of base to remove protons from hydrogen peroxide was also employed in reactions with $[Mn^{III}(salpn)(CH_3OH)_2](ClO_4)$, which does not form a complex with H_2O_2 in the absence of base.[50] In the reaction to yield $[Fe_6(O)_2(O_2)(O_2CPh)_{12}(H_2O)_2]$, one arm of one carboxylate on each $\{Fe_3O\}^{7+}$ unit is formally displaced by the incoming peroxo ligand. These ligands can then coordinate to an iron of the other triangular unit, providing two additional bridges between the original trinuclear iron species.[6] In **1**, a similar situation obtains, with acetates bridging from an iron of one trinuclear unit to an iron on the second triiron unit. Together with the three peroxo ligands, the additional three acetate bridges provide a total of six links between the two original $\{Fe_3O\}^{7+}$ units, with three carboxylates lost in the overall reaction to form the anion (Scheme 1). The cation is unreacted basic iron acetate.

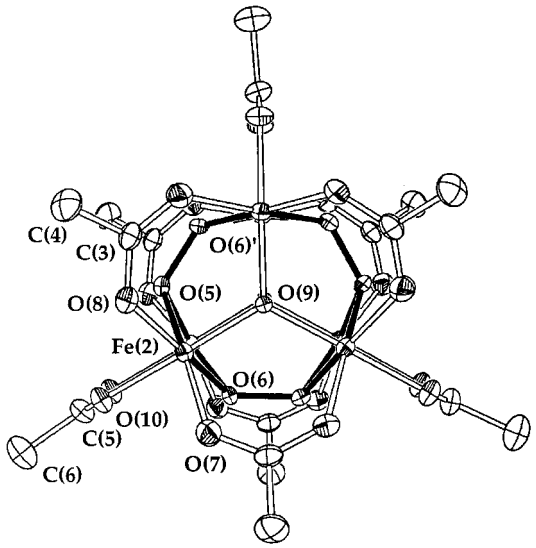

Figure 1. ORTEP diagram of the $[Fe_6(O)_2(O_2)_3(OAc)_9]^-$ anion viewed down the triangular faces of the Fe_6 prism. Bonds from the iron atoms to the peroxo ligands are depicted in bold.

The addition of $NaOCH_3$ to the slurry of basic iron acetate in acetone darkened the color and slightly increased the solubility of the starting material. When hydrogen peroxide was introduced, the color turned deep red. The reaction mixture was allowed to stir for 10 min, after which time any undissolved starting material was removed by filtration. Slow evaporation from acetone produced hexagonal, rod-like crystals which were stable in air. The reaction can be scaled up to 1.0 g of the basic iron acetate without sacrificing yield if the stirring time is lengthened to an hour.

Spectroscopy. The electronic spectrum of **1** in acetonitrile consists of a tail into the visible region with underlying bands which appear as weak shoulders at 425, 460, and 490 nm. The absence of a marked spectral feature at lower energy is interesting since most other ferric peroxo complexes have a well-defined ligand-to-metal charge transfer band generally appearing between 500 and 800 nm.[2,3,7,8] The μ^4-peroxo and/or the μ^3-oxo binding modes may be responsible for the lack of such a transition, since the spectrum of the related species, $[Fe_6(O)_2(O_2)(O_2CPh)_{12}(H_2O)_2]$, also displays only poorly defined shoulders (408, 456, and 534 nm) superimposed on a broad underlying tail in its electronic spectrum.[6] The O−O stretch was observed at 844 cm^{-1} in the Raman spectrum, a value which compares favorably with data for other iron-bound peroxo ligands,[2] particularly $[Fe_6(O)_2(O_2)(O_2CPh)_{12}(H_2O)_2]$, which absorbs at 853 cm^{-1}.[6]

Structure. The crystal lattice of **1**·8H_2O contains one trinuclear cation, one hexanuclear anion, and eight water molecules in the asymmetric unit. The highly symmetric nature of both the triiron(III) cation and hexairon(III) anion presumably facilitates crystallization in space group $P6_3/m$, and both clusters have crystallographically required D_{3h} symmetry. Two different views of the anion are presented in Figures 1 and 2; selected bond distances and angles are provided in Table 2. The structure of $[Fe_6(O)_2(O_2)_3(OAc)_9]^-$ is unprecedented, containing two basic iron acetate moieties linked in a face-to-face fashion by three peroxo bridges and three carboxylate bridges to form a triangular prism of six iron atoms. The peroxo bridges are unusual because

(47) Carlin, R. L. *Magnetochemistry*; Springer-Verlag: New York, 1986.
(48) O'Connor, C. J. *Prog. Inorg. Chem.* **1982**, *29*, 203−283.
(49) Doeuff, S.; Dromzee, Y.; Sanchez, C. *C. R. Acad. Sci. Paris* **1989**, *308*, 1409−1412.
(50) Larson, E. J.; Pecoraro, V. L. *J. Am. Chem. Soc.* **1991**, *113*, 3810−3818.

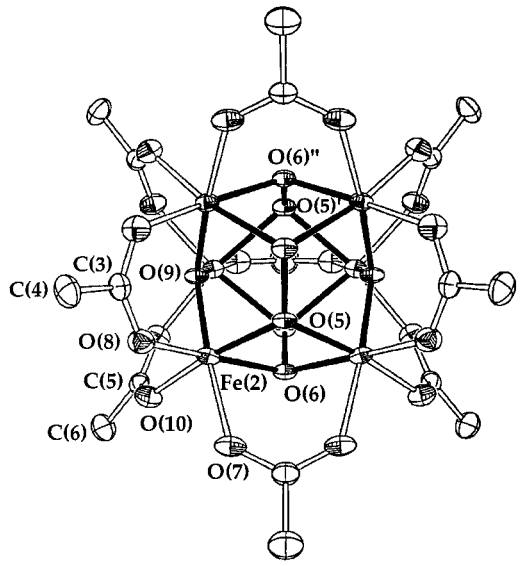

Figure 2. ORTEP diagram of the $[Fe_6(O)_2(O_2)_3(OAc)_9]^-$ anion viewed across a rectangular face of the Fe_6 prism.

Table 2. Selected Intramolecular Distances (Å) and Angles (Deg) Involving the Nonhydrogen Atoms of $[Fe_3(O)(OAc)_6(H_2O)_3][Fe_6(O)_2(O_2)_3(OAc)_6]\cdot 8H_2O$[a]

Intramolecular Distances (Å)			
Fe(1)−O(1)	1.893(1)	Fe(2)−O(7)	1.991(5)
Fe(1)−O(2)	1.996(6)	Fe(2)−O(8)	2.007(5)
Fe(1)−O(3)	2.005(5)	Fe(2)−O(9)	1.865(2)
Fe(1)−O(4)	2.049(7)	Fe(2)−O(10)	2.002(5)
Fe(2)−O(5)	2.047(4)	O(5)−O(6)′4	1.472(9)
Fe(2)−O(6)	2.106(5)		

Angles (deg)			
O(1)−Fe(1)−O(2)	94.7(2)	O(10)−Fe(2)−O(8)	90.0(2)
O(2)−Fe(1)−O(2)′1	91.9(5)	O(9)−Fe(2)−O(5)	90.2(3)
O(1)−Fe(1)−O(3)	94.9(2)	O(7)−Fe(2)−O(5)	171.6(2)
O(2)−Fe(1)−O(3)	87.8(3)	O(10)−Fe(2)−O(5)	86.4(2)
O(1)−Fe(1)−O(3)′1	94.9(2)	O(8)−Fe(2)−O(5)	90.4(2)
O(2)−Fe(1)−O(3)′1	170.4(3)	O(9)−Fe(2)−O(6)	90.3(3)
O(3)−Fe(1)−O(3)′1	90.9(4)	O(7)−Fe(2)−O(6)	91.5(2)
O(1)−Fe(1)−O(4)	178.8(2)	O(10)−Fe(2)−O(6)	85.3(2)
O(2)−Fe(1)−O(4)	86.2(2)	O(8)−Fe(2)−O(6)	170.2(2)
O(3)−Fe(1)−O(4)	84.3(2)	O(5)−Fe(2)−O(6)	80.8(2)
Fe(1)−O(1)−Fe(1)′2	120.0	Fe(2)−O(5)−O(6)′4	116.0(3)
Fe(1)−O(2)−C(1)	134.3(5)	Fe(2)−O(5)−Fe(2)′5	99.8(3)
Fe(1)−O(3)−C(1)′2	133.8(5)	Fe(2)−O(6)−O(5)′6	113.0(3)
O(7)−Fe(2)−O(9)	93.2(2)	Fe(2)−O(6)−Fe(2)′5	96.1(3)
O(9)−Fe(2)−O(10)	174.8(3)	Fe(2)−O(7)−C(3)′6	130.4(5)
O(7)−Fe(2)−O(10)	89.7(2)	Fe(2)−O(8)−C(3)	130.7(5)
O(9)−Fe(2)−O(8)	94.0(2)	Fe(2)−O(9)−Fe(2)′6	117.9(1)
O(7)−Fe(2)−O(8)	97.0(2)	Fe(2)−O(10)−C(5)	131.9(6)

[a] Symmetry transformations used to generate equivalent atoms: ′1, $x, y, -z + 1/2$; ′2, $-y + 1, x - y, z$; ′4, $-y, x - y, z$; ′5, $x, y, -z + 3/2$; ′6, $-x + y, -x, z$. Estimated standard deviations in the least significant figure are given in parentheses.

they are the first examples in iron chemistry of this ligand bound in a η^2-μ^4 mode and lying distinctly, by 1.05 Å, out of the plane of the metal atoms. The only other example of such a binding mode occurs in the peroxomolybdate, $[Mo_4O_{12}(O_2)_2]^{4-}$, where the O−O distance is 1.48 Å.[52]

Within the hexanuclear cluster, $[Fe_6(O)_2(O_2)_3(OAc)_9]^-$, the triiron components are relatively symmetrical, with distances of 2.007(5), 1.991(5), and 2.002(5) Å from Fe(2) to the carboxylate oxygen atoms and, as expected, a slightly shorter distance of 1.865(2) Å to the μ^3-oxo ion. The distances from Fe(2) to O(5) and O(6) of the peroxo ligand are elongated, at 2.047(4) and 2.106(5) Å, a feature not shared by the peroxo compound, $[Fe_6(O)_2(O_2)(O_2CPh)_{12}(H_2O)_2]$,[6] or in manganese complexes where a peroxo group bridges two metal centers in a η^2-μ^2 fashion.[40,41] In these other examples, the distances to the peroxo oxygens are similar to those of the rest of the coordination sphere. Elongation of the metal-peroxo bonds is, however, observed in the other example where an out-of-plane bridging mode occurs, $[Mo_4O_{12}(O_2)_2]^{4-}$, which suggests that the structural distortion is a result of this specific coordination mode.[51] The O(5)−O(6) peroxo distance of 1.472(9) Å agrees favorably with the value of 1.480(12) Å in $[Fe_6(O)_2(O_2)(O_2CPh)_{12}(H_2O)_2]$,[6] but is longer by about 0.06 Å than the O−O bonds in μ-1,2-peroxodiiron(III) complexes,[7−9] suggesting that attachment of four metals rather than two significantly weakens the O−O bond. This result also implies that protonation of the $Fe^{III}-O-O-Fe^{III}$ unit will weaken the bond, a reaction which might occur during subsequent chemistry of this intermediate in the carboxylate-bridged nonheme iron proteins.

The angles within the $\{Fe_3O\}^{7+}$ units of the hexanuclear cluster are more irregular than in the basic iron acetate cation (vide infra). At the Fe(2) center, angles between the carboxylate oxygens range from 90.0(2) to 97.0(2)°, with a trans angle of 174.8(3)°. Angles involving one peroxo and one carboxylate oxygen atom also range from 85.3(2) to 91.5(2)° for the cis angles and 170.2(2) to 171.6(2)° for the trans angles. The most acute angle around Fe(2) is that formed by oxygen atoms from two different peroxo ligands, O(5)−Fe(2)−O(6) = 80.8(2)°. The metal−metal distances in the cation and anion are slightly different. In the basic iron acetate cation, the Fe···Fe distance is 3.278(3) Å. In the hexanuclear anion, the comparable Fe···Fe distance in the $\{Fe_3O\}^{7+}$ subunit is shortened to 3.196(2) Å, and the distance between the closest irons of the two different subunits is even shorter at 3.131(2) Å. The two ionic components are connected in the solid state through a hydrogen bond from a terminal water ligand on the $\{Fe_3O\}^{7+}$ cation to the peroxo group on the anion, at a distance of 2.71(1) Å from the water to the closer peroxo oxygen atom, and 2.85(1) Å to the second peroxo oxygen atom.

The distances in the basic iron acetate cation agree well with average distances for the basic iron carboxylate unit,[52,53] with Fe−OAc bond lengths ranging from 1.996(6) to 2.005(5) Å and a slightly shorter value of 1.893(1) Å from Fe(1) to the bridging oxo ion. The O−Fe(1)−O angles of the carboxylates range from 87.8(3) to 91.9(5)° for the cis angles with trans angles of 170.4(3)°. Angles at Fe(1) from the carboxylates to the oxygen of the terminal water ligand, O(4), are slightly more acute at 84.3(2) and 86.2(2)°. The angles at Fe(1) of the carboxylates with the bridging oxo are 94.7(2)° and 94.9(2), and the trans angle to the terminal water ligand is nearly linear at 178.8(2)°. The octahedral environment at iron as well as the symmetry-required 120° angle at the central oxo ligand indicate the undistorted nature of this cationic species.

Mössbauer Properties. The Mössbauer spectrum of compound **1** was recorded at 180 K, 80 K, and 4.2 K. At all temperatures, the spectrum consists of a single, slightly asymmetric, quadrupole doublet consistent with high-spin ferric ion. The spectra at 80 K and 180 K were satisfactorily fit as a superposition of two unresolved symmetric quadrupole doublets with Lorentzian line shapes and an intensity ratio of 1:2 (Figure 3a). This fit is consistent with the X-ray crystallographic results, which reveal two unique iron coordination sites, one associated with the trinuclear cation, $[Fe_3O(OAc)_6(H_2O)_3]^+$, and the other

(51) Stomberg, R.; Trysberg, L.; Larking, I. *Acta Chem. Scand.* **1970**, *24*, 2678−2679.
(52) Blake, A. B.; Fraser, L. R. *J. Chem. Soc., Dalton Trans.* **1975**, 193−197.
(53) Holt, E. M.; Holt, S. L.; Alcock, N. W. *Cryst. Struct. Comm.* **1982**, *11*, 505−508.

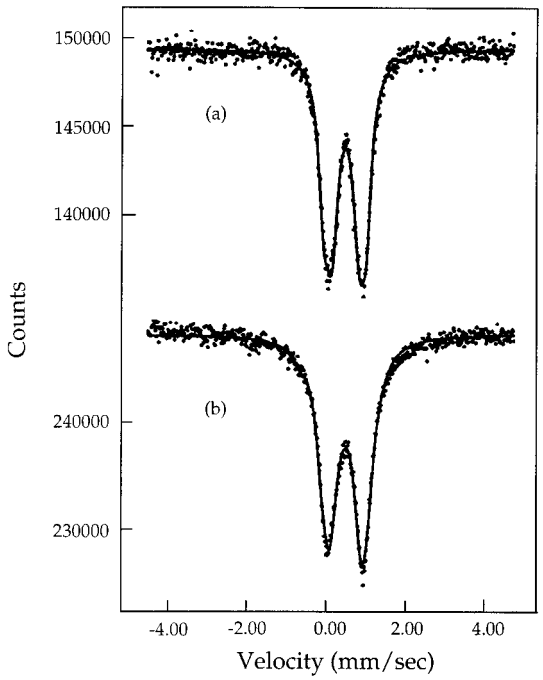

Figure 3. Mössbauer spectra of $[Fe_3O(OAc)_6(H_2O)_3][Fe_6(O)_2(O_2)_3(OAc)_9]$ at (a) $T = 80$ K and (b) $T = 4.2$ K. Solid lines are least-squares fits to the experimental data using Mössbauer parameters listed in Table 3. See text for discussion of fitting procedure.

Table 3. Mössbauer Parameters of $[Fe_3O(OAc)_6(H_2O)_3][Fe_6(O)_2(O_2)_3(OAc)_9]$

T (K)	δ^a (mm/s)	ΔE_q (mm/s)	H (kOe)	area (%)
180	0.46	1.07		36
	0.48	0.68		64
80	0.50	1.09		32
	0.51	0.70		68
4.2	0.51	1.16	3.8	34
	0.53	0.79	3.8	66

[a] Isomer shifts δ are relative to metallic iron at room temperature.

with the hexanuclear anion, $[Fe_6(O)_2(O_2)_3(OAc)_9]^-$. Fitted Mössbauer parameters are listed in Table 3.

There is a small temperature dependence of the isomer shifts, as expected from the second-order Doppler effect, and a small increase in the quadrupole splitting values with decreasing temperature. The smaller quadrupole splitting of about 0.7 mm/s falls well within the range of high-spin ferric ion compounds and is assigned to the hexanuclear iron cluster anion because it compares well with the value of about 0.6 mm/s previously observed in the hexanuclear cluster $[Fe_6O_2(OH)_2(O_2CPh)_{12}(OH_2)(1,4\text{-dioxane})]$.[17] The larger quadrupole splitting of about 1.0 mm/s is associated with the trinuclear cluster cation. This value is somewhat lower than the 1.5−2.0 mm/s range observed for oxo-bridged complexes,[54] but higher than the 0.45−0.71 mm/s range found for iron carboxylates.[55] The value compares favorably with that observed previously for the trinuclear cluster $[Fe_3O(TIEO)_2(O_2CPh)_2Cl_3]$, about 0.9 mm/s.[28]

At 4.2 K, the spectra exhibit a greater degree of asymmetry and broadening than could be reproduced by simply assuming the superposition of two symmetric quadrupole doublets (Figure 3b). The overall spectral shape suggests the onset of intermediate spin relaxation at low temperatures, which produces differential line broadening within a single quadrupole doublet. The inclusion of a small magnetic perturbation with an average

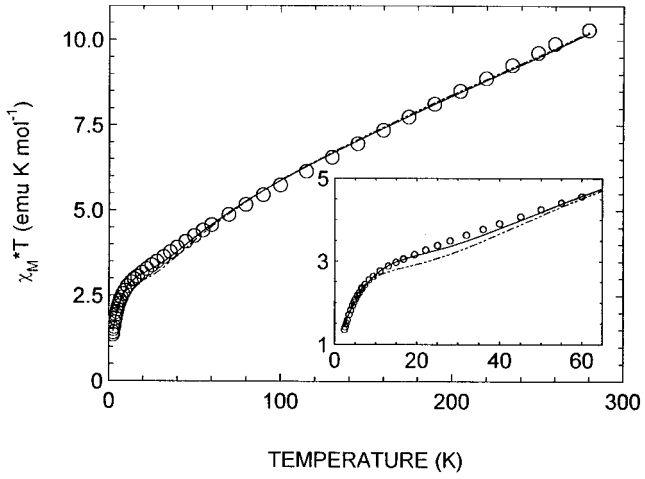

Figure 4. Temperature dependence ($\chi_M T$) of **1**. The solid line represents the best fit calculated for the parameters described in the text and the broken line corresponds to a fit with J_2 and J_3 fixed to zero. The inset is an expansion of the low-temperature region of the plot.

Scheme 2

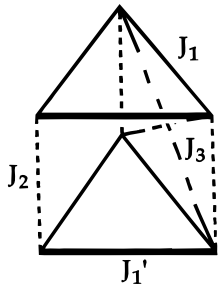

hyperfine magnetic field of ∼4 kOe and use of a negative sign for the principal component of the electric field gradient were necessary to fit the 4.2 K data (Table 3, Figure 3b). This result is consistent with the magnetic behavior of the compound, described below.

Magnetic Properties. The temperature dependence of the product $\chi_M T$ measured on a solid sample of **1** is plotted in Figure 4. The value of 9.90 per formula unit at the highest recorded temperature is much lower than that expected for nine uncoupled $S = {}^5/_2$ spins, 39.38 emu K mol^{-1}. This result indicates that relatively strong antiferromagnetic interactions are present, as expected for oxo-bridged polyiron(III) ions.[56] The $\chi_M T$ product decreases almost linearly with decreasing temperature down to ca. 10 K. Below this value, a faster decrease is observed, and at 2.45 K the value is 1.35 emu K mol^{-1}. Because no pathways for strong magnetic exchange between clusters are obvious from the crystal structure, the quantitative analysis of the magnetic behavior was carried out by assuming that the anion and cation are not interacting and that the magnetic susceptibility is given by the sum of contributions from a coupled six-spin system and a coupled three-spin system. In order to reduce the computation time, the irreducible tensor operators (ITO) approach was employed.[57] An attempt to reproduce the experimental behavior by assigning 3-fold symmetry to both cationic and anionic clusters and a total of four coupling constants, one for the cation, J_{tr}, and three for the anion (Scheme 2, $J_1 = J_{1'}$) was unsuccessful. This result is not surprising, since it is well known that an equilateral triangle of antiferromagnetically interacting $S = {}^5/_2$ spins, such as occurs in $\{Fe_3O\}^{7+}$, has a doubly

(54) Murray, K. S. *Coord. Chem. Rev.* **1974**, *12*, 1−35.
(55) Long, G. J.; Robinson, W. T.; Tappmeyer, W. P.; Bridges, D. L. *J. Chem. Soc., Dalton Trans.* **1973**, 573−579.
(56) Gorun, S. M.; Lippard, S. J. *Inorg. Chem.* **1991**, *30*, 1625−1630.
(57) Gatteschi, D.; Pardi, L. *Gazz. Chim. Ital.* **1993**, *123*, 231−240.

degenerate $S = {}^1/_2$ ground state.[58] Use of a model employing a single J value to reproduce the magnetic data of triangular clusters of iron(III) or chromium(III), even when crystallographic 3-fold symmetry is imposed, is generally inadequate.[58] The 2-fold degeneracy of the ground state makes the system sensitive to perturbations that can remove the degeneracy. Moreover, the coupling with lattice phonons can reduce the symmetry of the cluster while spin-orbit coupling gives rise to antisymmetric exchange. Considerable data reveal that inclusion of a second coupling constant, which implies C_2 rather than C_3 symmetry, allows the experimental results to be modeled quite well.[59]

In order not to overparameterize the model, we first reduced the symmetry in the hexanuclear cluster only (Scheme 2, $J_1 \neq J_{1'}$), and then introduced interactions mediated by the peroxo bridge (J_2 and J_3, Scheme 2), one at a time. By using the spin-Hamiltonian defined as $H = -2J|S_i \cdot S_j|$, the best fit was achieved with the following parameters: $J_1 = -51.3$, $J_{1'} = -33.5$, $J_2 = 0.8$ cm^{-1}, and setting $J_3 = 0$ for the hexanuclear cluster (Scheme 2) and $J_{tr} = -28.7$ cm^{-1} for the triangular cluster, with the g value fixed at 2.0 and $R = 3.6 \times 10^{-4}$. A reasonable fit ($R = 4.4 \times 10^{-4}$) was also obtained by fixing $J_2 = 0$ and using the parameters $J_1 = -47.3$, $J_{1'} = -31.9$, and $J_3 = -0.8$ cm^{-1} for the hexanuclear cluster. In both cases the ground state of the hexanuclear cluster had $S = 1$. A surprisingly poorer fit was achieved for $J_2 = J_3 = 0$ (Figure 4). Only a small improvement in the quality of the fits occurred by including a second J value for the trinuclear cation.

Although the analysis of the magnetic data of the present compound does not afford a unique set of the exchange parameters, owing to the number of possible interactions and the correlation among them, properties typical of spin-frustrated systems, several important findings were obtained. The value of J_{tr} agrees well with those reported for the many known triangular basic carboxylates of iron(III).[60] The interactions within the triangular faces of the hexanuclear anion are significantly stronger than those in the trinuclear cation, as expected from the longer Fe−O distance observed in the latter. In particular, the J value calculated by using a previously established magneto-structural correlation for oxo-bridged poly-iron(III) complexes[56] gives $J_1 = -48.8$ and $J_{tr} = -34.0$ cm^{-1}, in good agreement with the present results. A surprising result is the ferromagnetic nature of the interaction J_3, which corresponds to the μ-1,1-peroxo bridging mode. Since J_2 and J_3 (μ-1,2-peroxo bridging) are strongly correlated, we can only conclude that the hexanuclear cluster seems to have an $S = 1$ ground state and that the peroxo group is a poor mediator of magnetic exchange, contrary to expectations from the literature.[60] This result may be due to its long Fe−O distances and/or unusual bridging mode. We stress that, in our analysis, we have not taken into account antisymmetric exchange expected to be present and to influence the low-temperature susceptibility data. Only magnetic measurements on a single crystal would reveal, by the presence of a temperature-dependent magnetic anisotropy, the presence of such antisymmetric exchange. Unfortunately large enough crystals are not available.

Conclusions

The $[Fe_6(O)_2(O_2)_3(OAc)_9]^-$ anion contains a novel example of a cluster with three out-of-plane η^2-μ^2-peroxo groups and an elongated O−O bond compared to related η^2-μ^2-peroxo complexes. The Raman spectrum displays an O-O stretching band in the normal range for peroxo-bridged systems, but the electronic spectrum lacks a distinctive metal−peroxide charge transfer band in the 500−800 nm region. The Mössbauer spectra fit well to the statistical proportions of the number of iron atoms in the anion and its $[Fe_3O(OAc)_6(H_2O)_3]^+$ counterion, with an additional magnetic perturbation at low temperatures due to slow spin relaxation. Magnetic interactions between pairs of iron(III) centers in both the cation and anion are mediated chiefly by the oxo bridge, the values of the exchange coupling constants matching well the values calculated from an empirically derived expression relating Fe-O-Fe distance-geometry with J. The peroxo bridge does not contribute significantly to the magnetic exchange in the cluster anion. Given the increasing interest in peroxo-bridged di- and polymetallic intermediates in the catalytic reaction cycles of enzymes that metabolize dioxygen, the properties of this synthetic complex should be of value for comparison to those of the natural systems.

Acknowledgment. This research was supported by grants from the National Science Foundation and National Institute of General Medical Sciences. L.E.P. is grateful to the National Institutes of Health for a National Research Service Award (CA-59223). We are grateful to Dr. S. Herold, Dr. R. J. Lachicotte, and Ms. A. M. Barrios for helpful discussions. Raman spectra were obtained in the George R. Harrison Spectroscopy Laboratory at MIT.

Supporting Information Available: Complete listings of atomic coordinates, anisotropic thermal parameters, hydrogen atom coordinates, and bond distances and angles (5 pages). See any current masthead page for ordering and Internet access instructions.

JA963062R

(58) Cannon, R. D.; White, R. P. *Prog. Inorg. Chem.* **1988**, *36*, 195−298.

(59) Kitajima, N.; Tamura, N.; Amagai, H.; Fukui, H.; Moro-oka, Y.; Mizutani, Y.; Kitagawa, T.; Mathur, R.; Heerwegh, K.; Reed, C. A.; Randall, C. R.; Que, L., Jr.; Tatsumi, K. *J. Am. Chem. Soc.* **1994**, *116*, 9071−9085.

(60) Dong, Y.; Ménage, S.; Brennan, B. A.; Elgren, T. E.; Jang, H. G.; Pearce, L. L. ; Que, L. Jr., *J. Am. Chem. Soc.*, **1993**, *11*5, 1851−1859 and references cited therein.